environments

MDPI

Article

A Facile Approach to Preparing Molecularly Imprinted Chitosan for Detecting 2,4,6-Tribromophenol with a Widely Linear Range

Limei Huang, Yaqi Lu, Zhenyue Wu, Meishan Li, Shengchang Xiang, Xiuling Ma * and Zhangjing Zhang

College of Chemistry and Chemical Engineering, Fujian Provincial Key Laboratory of Advanced Materials Oriented Chemical Engineering, Fujian Provincial Key Laboratory of Polymer Materials, Fujian Normal University, Fuzhou 350007, China; lmhuanghx@126.com (L.H.); xlma@fjnu.edu.cn (Y.L.); zywu@126.com (Z.W.); limeishan2015@163.com (M.L.); scxiang@fjnu.edu.cn (S.X.); zjzhang@fjnu.edu.cn (Z.Z.)
* Correspondence: mxl502@163.com

Academic Editor: Yu-Pin Lin
Received: 12 February 2017; Accepted: 30 March 2017; Published: 2 April 2017

Abstract: The environmental pollution of 2,4,6-tribromophenol (TBP) has attracted attention. Based on an urgent need for the better provision of clean water, in situ determination of TBP is of great importance. Here, a facile and effective approach for detecting TBP is developed, based on coupling molecular imprinting technique with electrodeposition of chitosan (CS) on the gold electrode. The TBP imprinting CS film was fabricated by using CS as functional material and TBP as template molecule. The experiments show that the morphologies and electrochemical properties of the imprinted film sensor was different from non-imprinted film electrode. The current of the imprinted film was linearly proportional to the TBP concentration, with a wide linear range of 1.0×10^{-7} mol·L^{-1} to 1.0×10^{-3} mol·L^{-1}. By selecting drop-coating method as a reference for controlled trials with the same functional material, the results illustrated that the electrodeposition enjoyed a widely linear range advantage.

Keywords: 2,4,6-tribromophenol; chitosan; molecular imprinting; electrodeposition

1. Introduction

2,4,6-Tribromophenol (TBP) is an important chemical intermediate mainly used for the synthesis of brominated flame retardants (BFRs), medicines, pesticides, and preservatives. It has been detected in the environment, such as food packaging, seafood, and so on. There is also some information on TBP's toxicity and its effects on humans and the environment. For example, TBP caused an induction of aromatase activity in an human adrenocortical (H295R) cell line [1]; chronic exposures to environmental levels of tribromophenol impaired zebrafish reproduction [2]; TBP and the growth rate of fish displayed an obvious dose–effect relationship, with the minimum observable response concentration and unobservable response concentration of TBP being 0.64 and 0.32 mg·L^{-1}, respectively [3]. Therefore, the environmental pollution of TBP has attracted attention [4,5]. To detect TBP in the environment, methods were established using gas chromatography (GC) coupled with mass spectrometry (MS) or electron capture (EDC) with good sensitivity. However [6–8], these methods have some fatal shortcomings, as they require expensive instruments, have long analysis times, and are unsuitable for on-site monitoring.

The molecular imprinting technique (MIT)—also called the molecular template technique—has been proven to be an efficient way of making synthetic materials bearing selective molecular recognition sites [9]. Molecular imprinting polymers (MIPs) are prepared by a process that involves

the co-polymerization of functional monomers and crosslinkers around template molecules, then removing the template molecules from the polymer and rendering complementary binding sites capable of subsequent template molecule recognition [10]. With the development of MIT, MIPs have been an increasing concern for applications [11–15], particularly for use as the recognition element in the sensor [16–20]. Various fabrication methods for the imprinted sensor have been developed for satisfying the different detection purposes. Electropolymerization is one of the methods. It provides some advantages, including thickness control of the polymer layer (which is crucial to the sensing of the analyte), ability to attach the sensor film to electrode surfaces of any shape and size, and compatibility with combinatorial and high-throughput approaches critical for the commercial development of molecular imprinting [21–26].

Chitosan (CS) is a non-toxic biopolymer with good biocompatibility that is derived through a series of chemical treatments from the chitin components of the shells of crustaceans. It has several polar groups (e.g., –OH and $–NH_2$) which can act as electron donors. CS is soluble as the salt in various acids. It is chosen as the functional polymer for electrodeposition because CS amine salts are capable of contributing electrical conductance either in an aqueous solution or in a solid state [27]. In addition, considering the excellent reactivity of CS, it may be a versatile support material for the synthesis of imprinted polymers [28,29]. In addition, the imprinted CS polymer matrix shows gentle property and easy formation and elution for the molecular template [30], especially showing prospective applications in sensors [31].

Based on coupling MIT with the electrodeposition of CS, a facile approach for sensing TBP is developed in this study. The TBP imprinting CS film sensor was fabricated by using CS as functional material, TBP as template molecule, and H_2SO_4 as crosslinking agent and eluant. The detailed process involves the electrodeposition of CS on a gold electrode in TBP solution, crosslinking CS, and eluting the template molecule (TBP). The properties of the TBP imprinting electrode were investigated by electrochemical measurements. The experiments showed that there was almost no response to non-imprinted electrodes (absence of TBP template molecule during electrodeposition), while the current of the imprinted electrode was linearly proportional to the TBP concentration within the measured range from differential pulse voltammetry (DPV) measurements. Furthermore, the electrodeposited CS film-coated electrode with a widely linear range had the same performance as a nanoparticle-based system [32]. Based on the abundant amino, CS were introduced to bind with TBP, probably via N-H . . . O hydrogen bonds, which facilitates the recognition and selectivity for the analyte. In addition, drop-coating method was selected as a reference for controlled trials by using the same functional material: CS. The experiments show that the current of the electrode by drop-coating method was not linearly proportional to the TBP concentration within the measured range as determined by DPV. These results might illustrate that the electrodeposition is superior to the drop coating method. Our research provides an easy way to construct molecularly imprinted electro-polymers to sense phenolic pollutants. The fabrication of the sensor is illustrated in Figure 1.

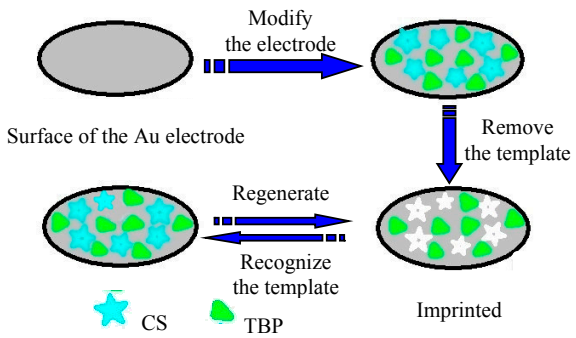

Figure 1. Schematic illustration of the 2,4,6-tribromophenol (TBP) electrochemical sensor fabrication. CS: chitosan [33].

2. Experimental

2.1. Instruments and Reagents

Morphology of the imprinted and non-imprinted films was characterized by scanning electron microscope (SEM, XL30ESEM-TMP, Eindhoven, The Netherlands). A CHI660E electrochemical workstation (CHI Instrument, Shanghai Chenhua Apparatus Company, Shanghai, China) was used for electrochemical measurements. The eluant was detected by UV-vis absorption spectroscopy (TU-1900, Beijing PERSEE Co., Ltd., Beijing, China) at 280 nm.

TBP (purity > 98%) was purchased from Aladdin. Chitosan (degree of deacetylation 80.0%–95.0%) was obtained from Sinopharm Chemical Reagent Co., Ltd. (Shanghai, China). All other chemicals were analytical reagent grade or better.

2.2. Preparation of TBP Imprinting Polymer Sensor (MIP/Au)

The 5.0 $g \cdot L^{-1}$ CS solution was prepared by dissolving CS in 1% acetic acid solution, and stored at 4 °C in a refrigerator.

Pretreatment step: Prior to modification, the Au electrode (3.0 mm in diameter)was polished with emery paper and chamois leather containing 0.3 μm and 0.05 μm Al_2O_3 slurry, respectively, and then thoroughly rinsed ultrasonically with ethanol and deionized water for 3 min in turn. Then, the electrode was cleaned by electrochemical cycling with the sweeping potential range from −0.3 V to 1.5 V in 0.5 $mol \cdot L^{-1}$ H_2SO_4 at 100 mV/s scan rate until stable cyclic voltammograms were obtained. Finally, the electrode was rinsed with deionized water and allowed to dry at room temperature.

Electrodeposition step: The deposition solution containing 1.0×10^{-4} $mol \cdot L^{-1}$ TBP with CS solution was first prepared. By employing a polished Au electrode as the working electrode, a platinum electrode as the counter electrode, and an Ag/AgCl electrode with saturated KCl as the reference electrode, the sediments were obtained using potentiodynamic cycling of potential for 30 scans in the range from −1.0 to 1.0 V at a scan rate of 100 mV/s. Then, the (TBP+CS)/Au was rinsed with deionized water and allowed to dry at ambient temperature for 2 h.

Cross-linking and elution step: The (TBP+CS)/Au was placed in 0.5 $mol \cdot L^{-1}$ H_2SO_4 solution by shaking. During soaking, both crosslink and removal of template take place at the same time. Thus, an electrochemical sensor based on CS molecularly imprinted film (MIP/Au) was developed.

The non-imprinting polymers sensor (NIP/Au) was prepared similarly to the MIP/Au, except that the template was absent in the electrodeposition step.

2.3. Measurements

A conventional three-electrode system was employed with a modified Au electrode as the working electrode, a platinum electrode as the counter electrode, and an Ag/AgCl electrode with saturated KCl as the reference electrode. All potentials reported in this article were referenced to the Ag/AgCl electrode. All measurements were carried out at room temperature.

Electrochemical impedance spectroscopy (EIS, Init E = 0.23 V, High Freq = 1×10^4 Hz, Low Freq = 1 Hz, Amplitude = 0.005 V)—which was used to investigate the charge transfer resistance of the film—was performed in 5.0 $mmol \cdot L^{-1}$ background solution $K_3[Fe(CN)_6]$ with 0.1 $mol \cdot L^{-1}$ KCl added as support electrolyte. DPV was utilized to evaluate the imprinting effect and the regeneration and stability. The DPV measurements were performed in a potential range between −0.2 V and 0.8 V, a modulation amplitude of 50 mV, a pulse width of 100 ms, and a step potential of 5 mV.

3. Results and Discussion

3.1. Preparation of MIP/Au Sensor

In this work, cyclic voltammetry was used to deposit CS with uniform and controlled thickness at gold electrode surfaces. The thicknesses of MIP films influence the quantity of the recognition

sites. Different numbers of cycles will form films with different thickness, which may finally affect the performance of the MIP film electrochemical sensor. With DPV, the response performance of MIPs/Au obtained by different cycle number were investigated in 5.0×10^{-6} mol·L^{-1} TBP. As shown in Figure 2, the greater the cycle number, the higher the response peak current values of TBP. When the cycle number was 30, it had maximum current values. Then, it showed a decreasing trend as the cycle number extended. The reason is that the longer electrodeposition time will form thicker films and more recognition sites were obtained [30], but the thicker films will also make much more trouble during the elution and rebinding of TBP in the center of films, which may finally result in a loss in sensitivity of the MIP sensor. So, 30 is the optimal electrodeposition cycle number.

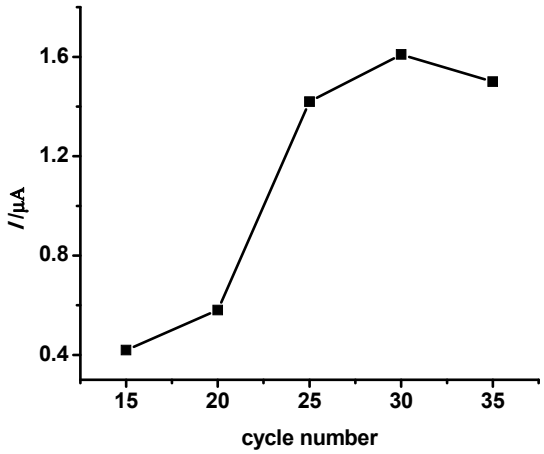

Figure 2. The response performance of molecular imprinting polymers (MIPs)/Au obtained by different cycle number in 5.0×10^{-6} mol·L^{-1} TBP (each point is representative of only one data point).

The cross-linking agent is one of the important factors in the preparation of molecularly imprinted membranes to improve the extent of cross-linking and maintain a better shape of the "memory" cavity structure. As in Reference [34], sulfuric acid was used as a cross-linking agent for the preparation of MIP/Au. CS polymer is a hydrophilic membrane showing a large swelling degree and lower selective property in the water. After cross-linking, the swelling degree of the CS MIP/Au decreased significantly. Using sulfuric acid as a cross-linking agent, the $-NH_2$ group in the CS membrane was cross-linked with SO_4^{2-} to improve the stability of the membrane structure and the ionic permeability [35]. In addition, the interaction between the CS and TBP would be destroyed under the condition of strong acidity during elution, which resulted in the leakage of TBP molecules from the stereoscopic cavity of the imprinted film.

3.2. Scanning Electron Microscopy

The morphologies of MIP/Au and NIP/Au were observed by SEM. There was a difference between the two sensors in Figure 3. The surface morphology of NIP/Au was compact (Figure 3A); after the template extraction, the imprinted sensor became rougher (Figure 3B), presumably caused by the change of macroscopic porosity of the MIP/Au after analyte extraction. Piletsky et al. [36] suggested that channels may be generated by template molecules, increasing the fraction of micropores in the polymer while also producing structures complementary to that of the template.

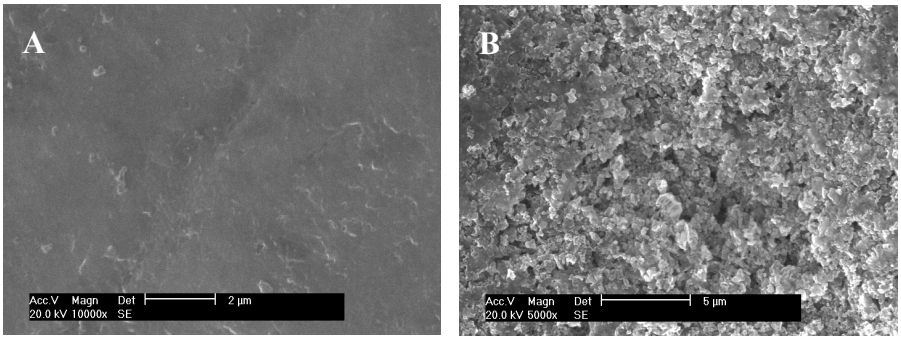

Figure 3. SEM micrographs of (**A**) NIP/Au; and(**B**) MIP/Au after the template extraction.

3.3. Supporting Electrolyte

DPV is relatively sensitive compared to CV, and was employed for the evaluation of the supporting electrolytes. It was performed after the bare electrode was immersed in different supporting electrolyte solutions with or without TBP. As shown in Figure 4A, they were almost the same in phosphate-buffered saline (PBS, pH ≈ 6) with or without TBP, while it was different in 0.3 mol·L^{-1} KCl (pH ≈ 6, Figure 4B). The difference in response between PBS and KCl may be due to the difference in electrolyte strength. KCl is a strong electrolyte that can improve the sensitivity of the detection of TBP, which is a weak electroactive substance. The 0.3 mol·L^{-1} KCl solution was selected for the analysis of sensor performance in the following sections.

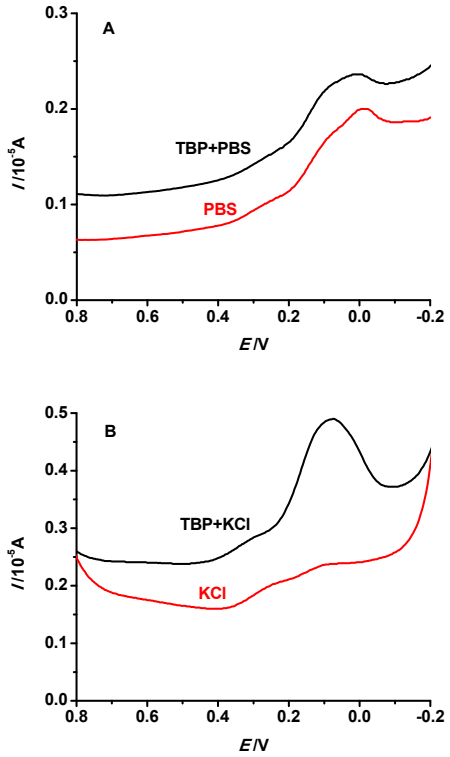

Figure 4. The differential pulse voltammetry (DPV) of the bare electrode in (**A**) phosphate-buffered saline (pH ≈ 6) with or without TBP; and (**B**) 0.3 mol·L^{-1} KCl (pH ≈ 6) with or without TBP.

3.4. Electrochemical Impedance Spectroscopy

EIS is an efficient tool for studying the films in terms of the interfacial electron transfer kinetics, and was used to investigate the change in resistance of different electrodes in 5.0 mmol·L^{-1} $K_3[Fe(CN)_6]$

with 0.1 mol·L^{-1} KCl. As shown in Figure 5, the impedance value of bare Au electrode is minimal (curve a), and the diameter of the semicircles of the NIP/Au electrode is larger than that of the MIP/Au. The results show that the imprinted one had a lower electron transport barrier, presumably due to the existence of porous binding sites after the template removal. The decrease in interfacial impedance is desirable, because it can decrease both the interfacial resistance drop of the electrode current and overpotential, leading to the enhancement of sensorial sensitivity [37].

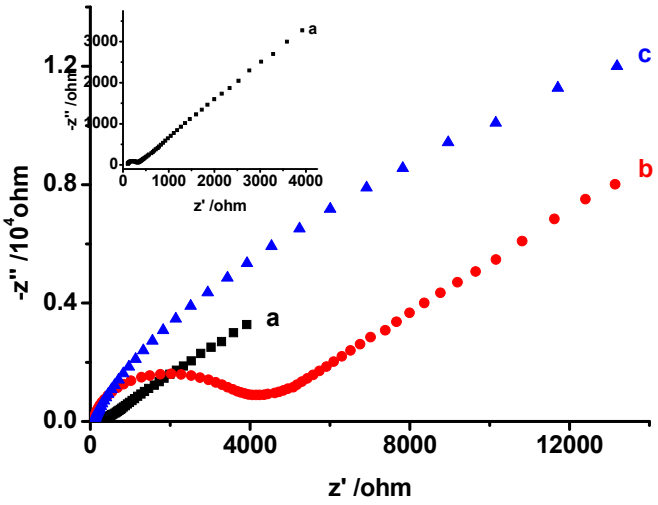

Figure 5. Electrochemical impedance spectroscopy (EIS) of different electrodes in 5.0 mmol·L^{-1} $K_3[Fe(CN)_6]$ with 0.1 mol·L^{-1} KCl: (**a**) bare electrode; (**b**) MIP/Au; (**c**) NIP/Au.

3.5. Performance of the Sensor

3.5.1. Effect of Imprinting

The specific selective capacity of MIP/Au was investigated by DPV with a comparison of NIP/Au in 5.0 × 10^{-6} mol·L^{-1} TBP with 0.3 mol·L^{-1} KCl. As shown in Figure 6, the adsorption capacity of MIP/Au is distinctly higher than NIP/Au because of the combination of physical adsorption and the specific recognition interaction. After removing the template molecules, the molecularly imprinted polymer can form specific binding sites that can recognize template molecules. Compared with aspecific adsorption, the adsorption capacity formed by the imprinting–extraction process was distinctly prominent.

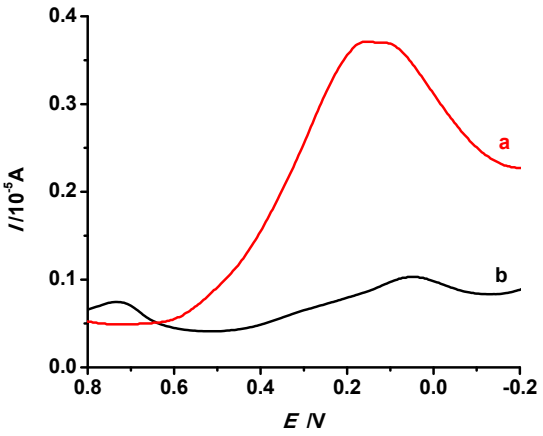

Figure 6. DPV of different sensors in 5.0 × 10^{-6} mol·L^{-1} TBP with 0.3 mol·L^{-1} KCl: (**a**) MIP/Au; (**b**) NIP/Au.

3.5.2. The Linear Range and Detection Limit of MIP/Au

DPV was also employed for the quantitative determination of TBP by immersing MIP/Au in solutions containing TBP of different concentration (1.0×10^{-3}, 1.0×10^{-4}, 1.0×10^{-5}, 1.0×10^{-6}, 1.0×10^{-7} mol·L^{-1}) with 0.3 mol·L^{-1} KCl. The cavities in the film were partially occupied by TBP, which led to the change of current signal. As shown in Figure 7A, the higher the concentration of TBP, the bigger the current value would be, which suggests that more and more binding sites in the film are occupied by TBP molecules. The peak current is linearly proportional to the TBP concentration in the range of 1.0×10^{-7} mol·L^{-1} to 1.0×10^{-3} mol·L^{-1} (shown in Figure 7B), with a correlation coefficient of 0.98692. The limit of detection (LOD, LOD = 3 S/m, where S is standard deviation of current value, and m is sensitivity, which is the slope of the linear equation) was 1.32×10^{-8} mol·L^{-1}. The CS film-coated electrode has a wide linear range, which is the same as a nanoparticle-based electrode made with a drop-coating method [21].

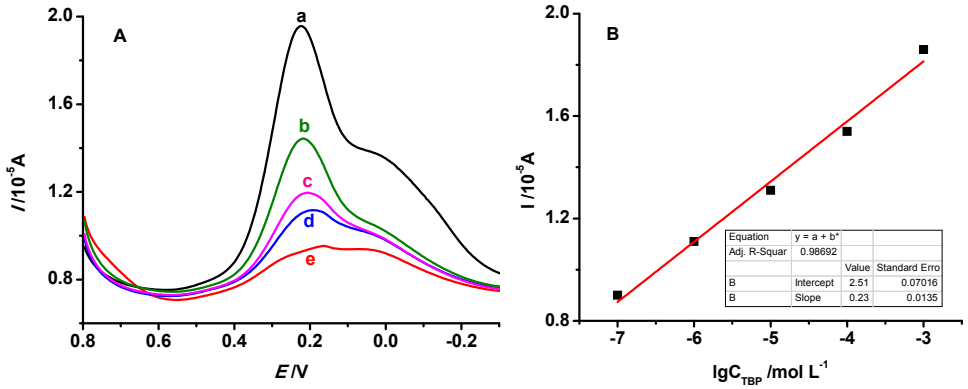

Figure 7. (**A**) DPV of MIP/Au in different concentrations of TBP by electrodeposition (a: 1.0×10^{-3}, b: 1.0×10^{-4}, c: 1.0×10^{-5}, d: 1.0×10^{-6}, e: 1.0×10^{-7} mol·L^{-1}); (**B**) The linear relation of *I*–lgC$_{TBP}$.

Using the same materials, drop-coating method was chosen as a reference. As shown in Figure 8, it was obvious that the peak current was not linearly proportional to the TBP concentration in the same range of electrodeposition. This may be due to the poor compatibility by drop-coating method. In addition, this method makes the sensor surface uniformity and film thickness uncontrollable, which affects the imprinting effect.

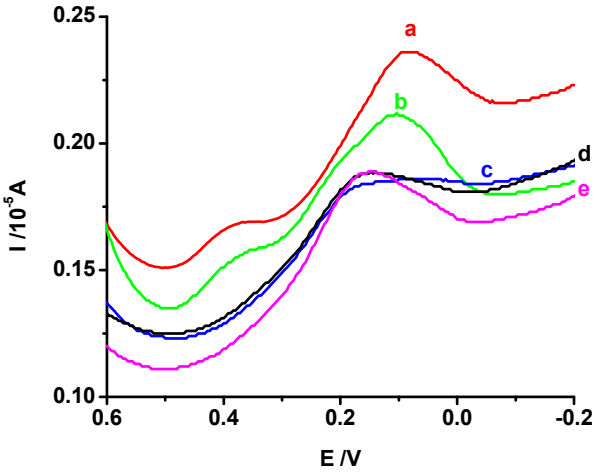

Figure 8. DPV of MIP/Au in different concentrations of TBP by drop-coating method (a) 1.0×10^{-3}; (b) 1.0×10^{-4}; (c) 1.0×10^{-5}; (d) 1.0×10^{-6}; (e) 1.0×10^{-7} mol·L^{-1}.

3.5.3. The Selectivity Performance of MIP/Au

Besides TBP, some species (i.e., 4-methyl-phenol and tert-butylhydroquinone) were employed as interference for selectivity tests of MIP/Au by the amperometric *i–t* curve (the initial potential: 0 V), which was utilized to evaluate the response to different substances. As shown in Figure 9, specific recognition of the template molecules (curve a) was the characteristic merit for MIP/Au. The sensor had selectivity towards the template molecule TBP. The selective recognition is based on the interaction between the template and the imprinting sites. The recognition sites formed in the polymerized film have the ability to distinguish target molecules through their size, shape, and functional group distribution [38].

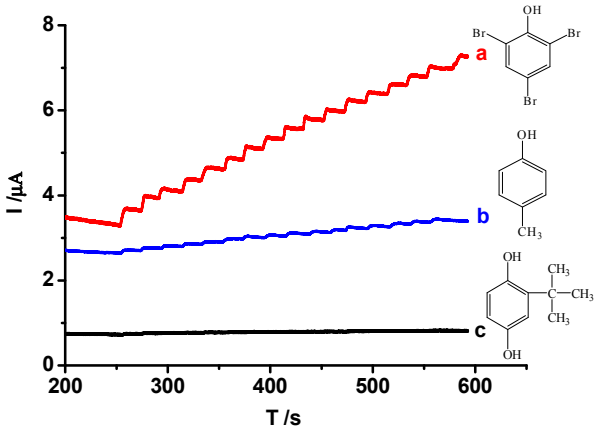

Figure 9. The amperometric *i–t* curve of MIP/Au in different solutions: (a) TBP; (b) 4-methyl-phenol; (c) tert-butylhydroquinone.

3.5.4. Regeneration and Stability

Regeneration is one of the most important properties for the application of the imprinted sensor. Therefore, the sensor was immersed in 0.5 mol·L^{-1} H_2SO_4 by shaking for 3 h, and back to the initial status. DPV was applied in solutions containing 5.0 × 10^{-3} mol·L^{-1} TBP and 0.3 mol·L^{-1} KCl. The cycle was repeated as described above. As shown in Figure 10, the current value of MIP/Au was much greater than NIP/Au, although the NIP/Au had almost no change. The current value of MIP/Au changed, but not much over five times, which indicates good regeneration performance. A small current change of MIP/Au may indicate that some recognition cavities might be blocked after regeneration or can be destroyed after rewashing, and thus they no longer matched the template molecule.

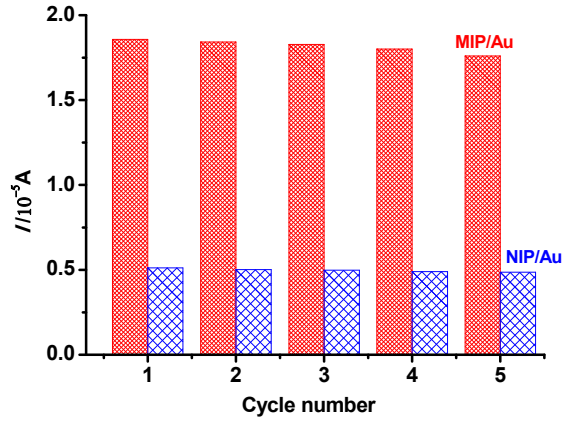

Figure 10. The regeneration of the MIP/Au and NIP/Au in 0.5 mol·L^{-1} H_2SO_4 by shaking for 3 h.

Similar to Reference [25], when not in use, the sensor can be simply protected in the electrode plastic cap filled with nitrogen, and stored at 4 °C in a refrigerator. The MIP/Au retained about 88% of its initial effect after 60 days of storage. The modified electrode exhibited good stability.

4. Conclusions

A new approach for the fabrication of a TBP–MIP sensor was presented by combining a molecular imprinting technique and the electrodeposition of a CS film on the gold electrode. The sensor was not only sensitive with a wide linear range, but also had good regeneration. In addition, the fabrication procedure is very simple, rapid, and inexpensive. Moreover, the experiments showed that the electrodeposition is superior to the drop coating method in the construction of the imprinted electrode. We believe that our strategy is instructive to the determination of other phenol pollutants.

Acknowledgments: The Authors gratefully acknowledge the financial supports of the National Natural Science Foundation of China (21207018, 21273033 and 21274022), Natural Science Foundation of Fujian Province (2015J01039), and the Open Project Program of the State Key Lab of Fuqing Branch of Fujian Normal University (KF1606).

Author Contributions: Xiuling Ma conceived and designed the experiments; Zhenyue Wu and Yaqi Ru performed the experiments; Meishan Li and Shengchang Xiang analyzed the data; Zhangjing Zhang contributed reagents/materials/analysis tools; Limei Huang wrote the paper.

Conflicts of Interest: The Authors declare no conflict of interest.

References

1. Cantón, R.F.; Sanderson, J.T.; Letcher, R.J.; Bergman, Å.; van den Berg, M. Inhibition and induction of aromatase (CYP19) activity by brominated flame. *Toxicol. Sci.* **2005**, *88*, 447–455. [CrossRef] [PubMed]
2. Deng, J.; Liu, C.S.; Yu, L.Q.; Zhou, B.S. Chronic exposure to environmental levels of tribromophenol impairs zebrafish reproduction. *Toxicol Appl. Pharm.* **2010**, *243*, 87–95. [CrossRef] [PubMed]
3. Zhang, S.; Liu, J.; Wang, L.; Yang, X.; Shi, L.; Liu, D. Endocrine disrupting effects of TBBPA and TBP on pelteobagrus fulvidraco. *J. Ecol. Rural Environ.* **2016**, *32*, 1012–1017.
4. Chuang, H.Y.; Joyce Ma, M.C.; Kim, J.S. Seasonal distribution of bromophenols in selected Hong Kong seafood. *J. Agric. Food Chem.* **2003**, *51*, 6752–6760. [CrossRef] [PubMed]
5. Belyea, J.; Gilvey, L.B.; Davis, M.F.; Godek, M.; Sit, T.L.; Lommel, S.A.; Franzen, S. Enzyme function of the globin dehaloperoxidase from *Amphitrite ornata* is activated by substrate binding. *Biochemistry* **2005**, *48*, 15637–15644. [CrossRef] [PubMed]
6. Blythe, J.W.; Heitz, A.; Joll, C.A.; Kagi, R.I. Determination of trace concentrations of bromophenols in water using purge-and-trap after in situ acetylation. *J. Chromatogr. A* **2006**, *1102*, 73–83. [CrossRef] [PubMed]
7. Polo, M.; Llompart, M.; Garcia-Jares, C.; Gomez-Noya, G.; Bollain, M.H.; Cela, R. Development of a solid-phase microextraction method for the analysis of phenolic flame retardants in water samples. *J. Chromatogr. A* **2006**, *1124*, 11–21. [CrossRef] [PubMed]
8. Huang, J.T.; Alquie, L.; Kaisa, J.P.; Reed, G.; Gilmor, T.; Vas, G. Method development and validation for the determination of 2,4,6-tribromoanisole, 2,4,6-tribromophenol, 2,4,6-trichloroanisole, and 2,4,6-trichlorophenol in various drug products using stir bar sorptive extraction and gas chromatography–tandem mass spectrometry detection. *J. Chromatogr. A* **2012**, *1262*, 196–204. [PubMed]
9. Osmani, Q.; Hughes, H.; McLoughlin, P. Probing the recognition of molecularly imprinted polymer beads. *J. Mater. Sci.* **2012**, *47*, 2218–2227. [CrossRef]
10. Chen, L.; Xu, S.; Lia, J. Recent advances in molecular imprinting technology: Current status, challenges and highlighted applications. *Chem. Soc. Rev.* **2011**, *40*, 2922–2942. [CrossRef] [PubMed]
11. Tiwari, M.P.; Prasad, A. Molecularly imprinted polymer based enantioselective sensing devices: A review. *Anal. Chim. Acta* **2015**, *853*, 1–18. [CrossRef] [PubMed]
12. Augusto, F.; Hantao, L.W.; Mogollon, N.; Braga, S. New materials and trends in sorbents for solid-phase extraction. *Trends Anal. Chem. TrAC* **2013**, *43*, 14–23. [CrossRef]

13. Zhang, C.; Li, F.; Wang, S.; Liu, Z.; Aisa, H.A. A new microemulsion approach for producing molecularly imprinted polymers with selective recognition cavities for gallic acid. *Anal. Methods* **2013**, *7*, 10256–10265. [CrossRef]
14. Ma, Y.; Pan, G.Q.; Zhang, Y.; Guo, X.Z.; Zhang, H.Q. Narrowly dispersed hydrophilic molecularly imprinted polymer nanoparticles for efficient molecular recognition in real aqueous samples including river water, milk, and bovine serum. *Angew. Chem. Int. Ed.* **2013**, *52*, 1511–1514. [CrossRef] [PubMed]
15. Huynh, T.P.; Chandra, B.K.C.; Sosnowska, M.; Sobczak, J.W.; Nesterov, V.N.; D'Souza, F.; Kutner, W. Nicotine molecularly imprinted polymer: Synergy of coordination and hydrogen bonding. *Biosens. Bioelectron.* **2015**, *64*, 657–663. [CrossRef] [PubMed]
16. Scognamiglio, V.; Antonacci, A.; Lambreva, M.D.; Litescu, S.C.; Rea, G. Synthetic biology and biomimetic chemistry as converging technologies fostering a new generation of smart biosensors. *Biosens. Bioelectron.* **2015**, *74*, 1076–1086. [CrossRef] [PubMed]
17. Gao, L.; Han, W.; Yan, Y.; Li, X.; Li, C.; Hu, B. A novel molecular imprinted nanosensor based quartz crystal microbalance for determination of kaempferol. *Anal. Methods* **2016**, *8*, 2434–2440. [CrossRef]
18. Tadi, K.K.; Motghare, R.V.; Ganesh, V. Electrochemical detection of sulfanilamide using pencil graphite electrode based on molecular imprinting technology. *Electroanalysis* **2014**, *26*, 2328–2336. [CrossRef]
19. Anirudhan, T.S.; Alexander, S. Design and fabrication of molecularly imprinted polymer-based potentiometric sensor from the surface modified multiwalled carbon nanotube for the determination of lindane (γ-hexachlorocyclohexane), an organochlorine pesticide. *Biosens. Bioelectron.* **2015**, *64*, 586–593. [CrossRef] [PubMed]
20. Luo, J.; Cong, J.; Liu, J.; Gao, Y.; Liu, X. A facile approach for synthesizing molecularly imprinted graphene for ultrasensitive and selective electrochemical detecting 4-nitrophenol. *Anal. Chim. Acta.* **2015**, *864*, 74–84. [CrossRef] [PubMed]
21. Blanco-López, M.C.; Lobo-Castañón, M.J.; Miranda-Ordieres, A.J.; Tuñón-Blanco, P. Electrochemical sensors based on molecularly imprinted polymers. *Trends Anal. Chem. TrAC* **2004**, *23*, 36–48. [CrossRef]
22. Malitesta, C.; Mazzotta, E.; Picca, R.A.; Poma, A.; Chianella, I.; Piletsky, S.A. MIP sensors—The electrochemical approach. *Anal. Bioanal. Chem.* **2012**, *402*, 1827–1846. [CrossRef] [PubMed]
23. Wang, Q.; Paim, L.L.; Zhang, X.; Wang, S.; Stradiotto, N.R. An electrochemical sensor for reducing sugars based on a glassy carbon electrode modified with electropolymerized molecularly imprinted poly-ophenylenediamine film. *Electroanalysis* **2014**, *26*, 1612–1622. [CrossRef]
24. Özcan, L.; Şahin, Y. Determination of paracetamol based on electropolymerized-molecularly imprinted polypyrrole modified pencil graphite electrode. *Sens. Actuators B Chem.* **2007**, *127*, 362–369. [CrossRef]
25. Cetó, X.; Saint, C.; Chow, C.W.K.; Voelcker, N.H.; Prieto-Simón, B. Electrochemical detection of *N*-nitrosodimethylamine using a molecular imprinted polymer. *Sens. Actuators B Chem.* **2016**, *237*, 613–620. [CrossRef]
26. Granado, V.L.; Gutiérrez-Capitán, M.; Fernández-Sánchez, C.; Gomes, M.T.; Rudnitskaya, A.; Jimenez-Jorquera, C. Thin-film electrochemical sensor for diphenylamine detection using molecularly imprinted polymers. *Anal. Chim. Acta* **2014**, *809*, 141–147. [CrossRef] [PubMed]
27. Twu, Y.K.; Chang, I.T.; Ping, C.C. Preparation of novel chitosan scaffolds by electrochemical process. *Carbohydr. Polym.* **2005**, *62*, 113–119. [CrossRef]
28. Guo, H.; Yuan, D.; Fu, G. Enhanced surface imprinting of lysozyme over a new kind of magnetic chitosan submicrospheres. *J. Colloid Interface Sci.* **2015**, *440*, 53–59. [CrossRef] [PubMed]
29. Liu, G.; Li, T.; Yang, X.; She, Y.; Wang, M.; Wang, J.; Zhang, M.; Wang, S.; Jin, F.; Jin, M.; et al. Competitive fluorescence assay for specific recognition of atrazine bymagnetic molecularly imprinted polymer based on Fe_3O_4-chitosan. *Carbohydr. Polym.* **2016**, *137*, 75–81. [CrossRef] [PubMed]
30. Chen, Y.P.; Liu, B.; Lian, H.T.; Sun, X.Y. Preparation and application of urea electrochemical sensor based on chitosan molecularly imprinted films. *Electroanalysis* **2011**, *23*, 1454–1461. [CrossRef]
31. Duan, H.; Li, L.; Wang, X.; Wang, Y.; Li, J.; Luo, C. CdTe quantum dots@luminol as signal amplification system for chrysoidine with chemiluminescence-chitosan/graphene oxide-magnetite-molecularly imprinting sensor. *Spectrochim. Acta A* **2016**, *153*, 535–541. [CrossRef] [PubMed]
32. Ma, X.; Wu, D.; Huang, L.; Wu, Z.; Xiang, S.; Chen, S. Sensing 2,4,6-tribromophenol based on molecularly imprinted technology. *Monatsh. Chem.* **2015**, *146*, 485–491. [CrossRef]

33. Wu, Z. *Preparation of Tribromophenol Molecularly Imprinted Sensor [D]*; Fujian Normal University: Fuzhou, China, 2014.
34. Ma, X.; Chen, R.; Zheng, X.; Youn, H.; Chen, Z. Preparation of molecularly imprinted CS membrane for recognizing naringin in aqueous media. *Polym. Bull.* **2011**, *66*, 853–863. [CrossRef]
35. Cui, Z.; Xiang, Y.; Zhang, T. Investigation on proton conductivity behavior of sulfuric acid cross-linked chitosan membrane. *Acta. Chim. Sinica* **2007**, *65*, 1902–1906.
36. Piletsky, S.A.; Panasyuk, T.L.; Piletskaya, E.V. Receptor and transport properties of imprinted polymer membranes—A review. *J. Membr. Sci.* **1999**, *157*, 263–278. [CrossRef]
37. Li, S.; Du, D.; Huang, J.; Tu, H.; Yang, Y.; Zhang, A. One-step electrodeposition of a molecularly imprinting chitosan/phenyltrimethoxysilane/AuNPs hybrid film and its application in the selective determination of p-nitrophenol. *Analyst* **2013**, *138*, 2761–2768. [CrossRef] [PubMed]
38. Liu, Y.T.; Deng, J.; Xiao, X.L.; Ding, L.; Yuan, Y.L.; Li, H.; Li, X.T.; Yan, X.N.; Wang, L.L. Electrochemical sensor based on a poly(para-aminobenzoic acid) film modified glassy carbon electrode for the determination of melamine in milk. *Electrochim. Acta* **2011**, *56*, 4595–4602. [CrossRef]